Applied Catalysis B: Environmental 331 (2023) 122708

Contents lists available at ScienceDirect

Applied Catalysis B: Environmental

journal homepage: www.elsevier.com/locate/apcatb

On the relevant role of iron complexation for the performance of photo-Fenton process at mild pH: Role of ring substitution in phenolic ligand and interaction with halides

Ivan Vallés [a], Iván Sciscenko [a], Margarita Mora [b], Pau Micó [c], Ana M. Amat [a], Lucas Santos-Juanes [a], Javier Moreno-Andrés [a,d], Antonio Arques [a,*]

[a] Grupo de Procesos de Oxidación Avanzada, Departamento de Ingeniería Textil y Papelera, Universitat Politècnica de València, Campus de Alcoy, Alcoy, Spain
[b] Grupo de Procesos de Oxidación Avanzada, Departamento de Matemática Aplicada, Universitat Politècnica de València, Campus de Alcoy, Alcoy, Spain
[c] Departamento de Informática de Sistemas y Computadores, Universitat Politècnica de València, Plaza Ferrándiz y Carbonell s/n, 03801 Alcoy, Spain
[d] Department of Environmental Technologies, Faculty of Marine and Environmental Sciences, INMAR-Marine Research Institute, CEI·MAR, International Campus of Excellence of the Sea, University of Cadiz, Spain

ARTICLE INFO

Keywords:
Chloride
Fluoride
Iron chelates
Phenolic compounds
Photo-Fenton

ABSTRACT

In this work, a systematic study on the effect of Fe(III) complexation by phenolic derivatives with different substitution on photo-Fenton has been carried out. Solutions containing a mixture of six pollutants (30 $mg{\cdot}L^{-1}$) were treated by solar simulated photo-Fenton ([Fe(II)] = 0.09 $mmol{\cdot}L^{-1}$, [H_2O_2] = 4.29 $mmol{\cdot}L^{-1}$, pH = 5, [Ligand] = 0.227 $mmol{\cdot}L^{-1}$. The efficiency of ligand increased with the presence of -OH groups (mainly in ortho-position), while the reverse was true for -COOH and -OCH_3. This was correlated with the ability of the ligands to reduce Fe(III) to Fe(II). Catechol (CAT) supressed the interference of chlorides at [NaCl] = 30 mg/L^{-1} by complexing iron(III) thus preventing formation of $FeCl_2^+$, as 85% of Fe(III) was found as $Fe(CAT)_3$ according to mathematical calculations. Hence, effluent matrix, including anions and organic pollutants, has a remarkable effect on iron speciation and a it should be considered when determining reaction conditions.

1. Introduction

Iron based processes for wastewater treatment are gaining momentum [1]. Although this ubiquitous and inexpensive metal has been used since long time ago in processes such as coagulation, in last decades novel uses have been developed: iron-containing catalysts for heterogeneous pollutants oxidation [2,3], highly valent [4] and zero-valent iron processes [5,6] and Fenton-related treatments [7]. The chemistry of iron is very complex; this element exhibits different oxidation states, can form coordination compounds with a wide range of organic and inorganic ligands, including OH^-, and the solubility of iron species in water differs depending on their nature, also showing a strong pH dependence. For instance, in marine ecosystems, more than 99% of the dissolved iron has been reported to be complexed by organic ligands [8], especially by humic substances, which constitute the major fraction among dissolved organic matter and have demonstrated a high affinity for iron [9]. Thus, iron complexation has important implications on the performance of iron-based processes, in particular for photo-Fenton, where the key step involves a ligand to metal charge transfer transition to reduce Fe(III) into Fe(II) [10].

Briefly, the Fenton process is based on the Haber-Weiss reaction, which produces highly oxidative species via H_2O_2 decomposition in the presence of iron salts. Fenton-based treatments have been demonstrated to be very efficient for the removal of a wide range of pollutants [11], although their performance strongly depends on the composition of the water matrix. In order to understand the nature of these effects, the manifold of reactions (1)-(7) has to be considered. In the absence of light, process occurs via Eqs. (1) and (2), (Fenton process), and the reaction rate is limited by the second step. Upon irradiation, the process can be highly accelerated as more efficient Fe(II) regeneration occurs via reactions (3)-(5), when no other ligands than OH^- are present. A clear pH dependence is observed, as the concentration of $Fe(OH)^{2+}$ reaches its maximum at pH = 2.8, and reaction (5) becomes predominating, thus regenerating Fe(II). However, at higher pH, reaction (4) is favoured, deactivating Fe(III) as catalyst by formation of iron oxides and/or hydroxides unable to take part in the Fenton process. In the presence of

* Corresponding author.
E-mail address: aarques@txp.upv.es (A. Arques).

https://doi.org/10.1016/j.apcatb.2023.122708
Received 23 November 2022; Received in revised form 28 March 2023; Accepted 29 March 2023
Available online 31 March 2023
0926-3373/© 2023 The Author(s). Published by Elsevier B.V. This is an open access article under the CC BY-NC-ND license (http://creativecommons.org/licenses/by-nc-nd/4.0/).

other iron ligands (L), reactions (6) and (7) should be considered, when L is able to displace the OH^-. Then, different behaviours can be obtained depending on the properties of FeL. If this complex is able to regenerate Fe(II) by reducing Fe(III), then the photo-Fenton process can be kept efficient even at different pH domains. In fact, this is a methodology employed to extend the applicability of photo-Fenton towards neutral media [12–15]. However, if the FeL complex is not active, or the generated species are less efficient than·OH, change of OH^- by L results in a loss of efficiency of photo-Fenton. This is the case of chlorides, where the formation of chlorinated iron(III) complex instead of $Fe(OH)^{2+}$ has a detrimental effect on (photo)-Fenton [16–18]. This is one of the reasons why the application of photo-Fenton in highly saline media, such as seawater, has received minor attention from researchers [19–22].

$$Fe^{2+} + H_2O_2 \rightarrow Fe^{3+} + \cdot OH + OH^- \quad (1)$$

$$Fe^{3+} + H_2O_2 \rightarrow Fe^{2+} + \cdot O_2H^- \quad (2)$$

$$Fe^{3+} + OH^- \rightarrow Fe(OH)^{2+} \quad (3)$$

$$Fe(OH)^{2+} + OH^- \rightarrow \text{catalyst inactivation} \quad (4)$$

$$Fe(OH)^{2+} + h\upsilon \rightarrow Fe^{2+} + \cdot OH \quad (5)$$

$$Fe^{3+} + L \rightarrow FeL^{3+} \quad (6)$$

$$FeL^{3+} (+ h\upsilon) \rightarrow Fe^{2+} + L^{\cdot} \quad (7)$$

In addition to this, some organic species, commonly considered as pollutants, have demonstrated the ability to form iron(III) complexes and thus, to modify the photo-Fenton mechanism [23]. For instance, antibiotics such as fluoroquinolones can be degraded via photo-Fenton efficiently at pH = 5 [24], some organic fertilizers can enhance photo-Fenton at circumneutral pH [25,26] and the ability of phenols to complex iron [27] results in a shift of the optimum pH towards higher values in effluents with high phenolic content, such as food or cork industry [28,29]. This fact indicates that cross effects among those pollutants might be important on the photochemical fate of contaminants of emerging concern (CECs), but they have been commonly neglected.

A few studies have assessed phenolic substances as promoters of Fenton-based reactions, using compounds such as gallic acid [30,31], protocatechuic acid [32], caffeic acid [33] or catechol [34,35]. Also, benzoic acid derivatives, and their oxidation byproducts have been demonstrated to favour (photo)-Fenton processes [36,37]. In addition to this, macromolecules such as humic and humic-like substances contain important amounts of phenolic moieties in their structures, what can explain their ability to enhance photo-Fenton at mild conditions [38,39]. Recently, the correlation of substitution on 1,2-dihydroxybenzenes and their efficiency as auxiliaries for photo-Fenton has been reported [40] and mechanistic issues for the interaction between Fe(III) and polyphenols has been reviewed focusing in their application in Fenton systems [41]. Briefly, a one-electron pathway between Fe(III) and the ligand has been described for *o*-diphenols to form Fe(II) and a semiquinone; then, another electron is transferred from the semiquinone to oxygen, to form superoxide radical and the *o*-quinone [42]. Finally, despite treatments based on addition of these substances should be, in general, ruled out because of their toxicity, phenolic moieties are ubiquitously present, for instance in a wide range of pollutants, and might play a relevant role that has been scarcely considered.

The results above reported proof that the use of phenolic compounds as ligands for iron is a hot topic that has deserved important attention from researchers, but there are still some issues that remains to be clarified. For instance, as far as we know, there is a lack of a systematic, integrative and comparative study on the effect of the nature, number and position of the substituents on the aromatic ring on the efficiency of (photo)-Fenton. These parameters might be of importance, in order to form the Fe(III)-L complex and to favour or hinder the electron-transfer process required to reduce Fe(III) into Fe(II). In addition to this, most experiments have been performed with a single pollutant, which might interact itself with iron and drive to misleading results, which can be lessened by using a group of pollutants with different structures. Finally, the competitive effect between organic and inorganic ligands (e.g chlorides) remains unexplored, and might be of paramount importance, as salts are ubiquitously present in real water matrices.

With this background, the main goal of this work is to assess the enhancement of photo-Fenton processes at pH = 5 by different phenols and benzoic acid derivatives (see Fig. 1 for structures): catechol (CAT), resorcinol (RES), p-hydroxyquinone (PHQ), phenol (PHE), gallol (GAL), p-hydroxybenzoic acid (PHB), protocatechuic acid (PRO), gallic acid (GAA), vanillic acid (VAN), veratric acid (VER), salicylic acid (SAL) and phthalic acid (PHT). Despite addition of these substances to reaction mixtures should be disregarded because of their toxicity, these moieties can be found in many families of pollutants or macromolecules, as stated above, and this study can lead to a better understanding of (photo)-Fenton-(like) when these functional groups are present. The combined effect of selected ligands with two ubiquitous inorganic species (chloride and fluoride) has also been investigated. A mixture of six CECs has been employed as target for the photo-Fenton processes, namely acetamiprid (insecticide), amoxycillin (antibiotic), acetaminophen (analgesic), caffeine (stimulating agent), clofibric acid (metabolite of clofibrate, also employed as herbicide) and carbamazepine (psychiatric drug). This is a representative mixture of xenobiotics present in effluents that has been successfully employed in previous studies [38,43] and allows to approach to real situations where mixtures of pollutants are commonly present, and avoid to rely on the particular behaviour of a single chemical, that might not be representative (e.g by interacting with Fe (III)).

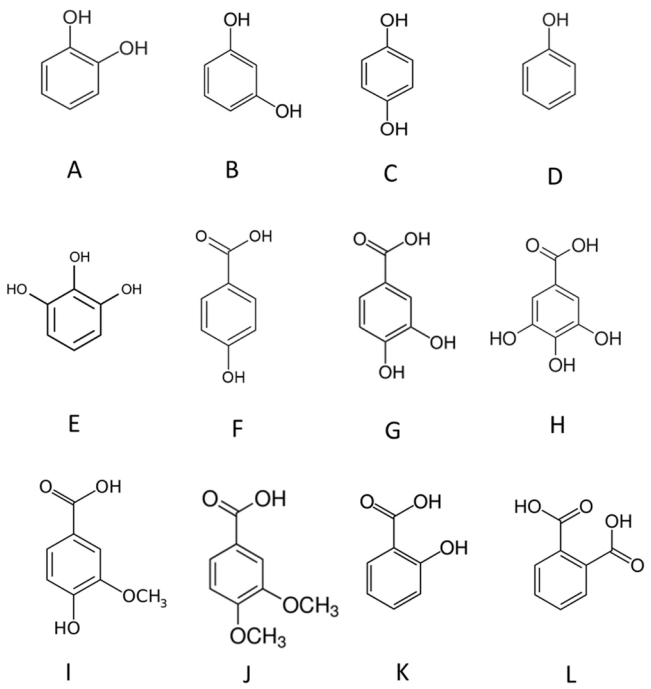

Fig. 1. Chemical structures of phenolic derivatives used as ligands in this work: catechol, CAT (A), resorcinol, RES (B), p-hydroxyquinone, PHQ (C), phenol, PHE (D), gallol, GAL (E), p-hydroxybenzoic acid, PHB (F), protocatechuic acid, PRO (G), gallic acid, GAA (H), vanillic acid, VAN (I), veratric acid, VER (J), salicylic acid, SAL (K) and phthalic acid, PHT (L).

2. Material and methods

2.1. Reagents

High purity (>98%) reagents used as target pollutants (acetamiprid, acetaminophen, caffeine, amoxicillin, clofibric acid, carbamazepine) or phenolic derivatives (Fig. 1) used as ligands (PHE, CAT, RES, PHQ, GAL, PHB, PRO, GAA, VAN, VER, SAL and PHT) were supplied by Sigma-Aldrich.

Fenton-like reactions were carried out with iron(II) sulfate ($FeSO_4 \cdot 7\,H_2O$) and hydrogen peroxide (H_2O_2, 30% w/w), both of them purchased from PanReac. Methanol, formic acid and acetonitrile (all of them HPLC grade), sulphuric acid, sodium hydroxide, ascorbic acid, *o*-phenantroline and ammonium metavanadate were purchased from PanReac. Water employed in all solutions was of Milli-Q grade. For those experiments with inorganic anions, NaCl or NaF (99%, Panreac) was added to Milli-Q water.

2.2. Reactions

The target solution consisted of a mixture of the six CECs (acetamiprid, acetaminophen, caffeine, amoxicillin, clofibric acid and carbamazepine) with an initial concentration of 5 $mg \cdot L^{-1}$ each. This concentration ensures reliable kinetics and allows comparisons between the different tested conditions. When required, saline water was prepared by adding NaCl or NaF as sources of Cl^- and F^-, respectively, to Milli-Q grade water.

Experiments were performed in 250 mL cylindrical open glass reactors. The reactor was loaded with the solution containing the six CECs together with 5 mg L^{-1} of iron (0.089 mmol L^{-1}), a concentration typically employed in this type of experiments [33,38]. The pH was adjusted to 5 by addition of diluted H_2SO_4 or NaOH. Then, when required, the complexing agent was added at a concentration of 0.227 $mmol \cdot L^{-1}$; this molar ratio (ca: 1:2.5) is in the range that reported in other studies [30,31,34,41,44]. Hydrogen peroxide was added at 146 $mg \cdot L^{-1}$ (4.29 $mmol \cdot L^{-1}$), which is the stoichiometric amount to mineralize the mixture of CECs assuring that i) the effect of the amount of H_2O_2 added to the reaction medium is normalized, and ii) the exhaustion of H_2O_2 is avoided [38,45].

Irradiation was performed with a solar simulator (Oriel Instruments, Model 81160 equipped with a 300 W xenon lamp). Specific glass filters were used to cut off the transmission of wavelengths $\lambda < 300$ nm. The UV-A irradiance (315–400 nm) was 32 $W \cdot m^{-2}$. Irradiation started simultaneously to the addition of hydrogen peroxide and was carried out for up to one hour. Samples were periodically taken from the solution for analysis; those to be analysed by HPLC were diluted 1:1.5 with methanol to quench the excess of peroxide in order to stop the Fenton process. The pH was monitored throughout the process and values were systematically above 4. Dark-Fenton reactions were performed at the same experimental conditions, but in the absence of radiation. Also, controls were carried out with a representative ligand, i.e., CAT. Thus, photolysis of the pollutants mixture in the presence of Fe(II), CAT, Fe(II)/CAT, H_2O_2, as well as their corresponding blank controls were contemplated. All reactions were repeated at least twice; if results were not coincident, a third run was performed.

2.3. Analytical measurements

The concentration of each CEC was determined by HPLC (Hitachi Chromaster chromatograph; VWR) equipped with a UV/Vis detector. A Prevail Hichrom column (C18-Select; 250 ×4.6 mm; 5 μm) was employed as stationary phase. The mobile phase (flow rate of 1 $mL \cdot min^{-1}$) consisted of a binary mixture of solvents A (acetonitrile) and B (10 mM formic acid aqueous solution). The linear gradient was operated from 10% A to 90% A in 25 min. Re-equilibration time was 7 min. The wavelength used for the quantitation of the CECs was 225 nm. Retention times are the following: amoxicillin (6.1 min), acetaminophen (9.3 min), caffeine (10.1 min), acetamiprid (13.8 min), carbamazepine (16.5 min) and clofibric acid (24.5 min).

The cumulative remaining concentration of pollutants (ΣC, where C is the concentration of each pollutant) was used as response, as a mean to minimize the individual behaviour of each target compound. Removals were expressed as relative values ($\Sigma(C/C_0)$), where C_0 is the initial concentration of pollutants.

The concentration of iron species in the water was measured according to the 1,10-phenanthroline standardized spectrometric procedure (ISO 6332:1988) using a UH5300 – Hitachi Spectrophotometer. The efficiency of Fe(III) reduction at pH 5 by different ligands was evaluated by adding CAT, PHQ, VAN and PHT (each in concentration 0.227 $mmol \cdot L^{-1}$) to a solution of Fe(III) at 5 mg L^{-1} (added as $Fe(ClO_4)_3$) with 1, 10-phenanthroline at 0.5 mg L^{-1}. Absorbance at 510 nm over time was measured for 2 h. Consumption of hydrogen peroxide was determined following a modification of the metavanadate method [46].

Spectra of Fe(III) and their complexes with different ligands were measured with a UH5300 – Hitachi Spectrophotometer in the range 300–600 nm. The pH of the solution was 5, the concentration of iron was 0.089 $mmol \cdot L^{-1}$ and that of the ligand was 0.227 $mmol \cdot L^{-1}$. A quartz cell with an optical pathway of 1 cm was employed for measurements.

2.4. Iron speciation

Calculations on Fe(III) speciation were performed with CAT as representative ligand. Calculations were developed by means of MATLAB 2020a through "vpasolve" function, based on previous work [47]. The equation describing the processes (8), the respective accumulative stability constants, βi, (Eq. (9)), and mass balances (Eqs. (10) and (11)) for total Fe(III) and ligands, respectively are the following:

$$xFe^{3+} + yL^{m} \leftrightarrow Fe_xL_y^{3x\text{-}ym} \tag{8}$$

$$\beta_{x,y} = \frac{\left[Fe_xL_y^{3x-ym}\right]}{\left[Fe^{3+}\right]^x[L^m]^y} \tag{9}$$

$$[\boldsymbol{Fe}total] = \left[Fe^{3+}\right] + \sum x\beta_{x,y}\left[Fe^{3+}\right]^x[L^m]^y \tag{10}$$

$$[\boldsymbol{L}total] = [L^m] + \sum y\beta_{x,y}\left[Fe^{3+}\right]^x[L^m]^y \tag{11}$$

where "y" and "m" are the stoichiometric and charge number, respectively, of the ligand L (i.e. OH^-, Cl^- or CAT), and "x" is the stoichiometry number of Fe^{3+} in the complex. The employed stability constants for the Fe(III)-chloride constants were taken from De Laat and Le [48]; in the case of catechol the $Fe(CAT)_3^{3-}$ complex has been considered and the constants were taken from Perron and Brumaghim [49].

2.5. Volumetric rate of photon absorption calculation

The volumetric rate of photon absorption was calculated following the procedure reported by Cabrera Reina et al. [50]. First, the spectral averaged specific absorption coefficient k ($mM^{-1}\ m^{-1}$) of the solution was determined according to Eq. (12), where I_λ ($W\ m^{-2}$) is the lamp power at each wavelength [51] and ε_λ ($mM^{-1}\ m^{-1}$) is the specific absorption coefficient of the solution, obtained from the corresponding spectra (shown in Fig. S1) The k was calculated for the UVA region ($\lambda_{min} = 325$ nm and $\lambda_{max} = 385$ nm), which is the range usually considered for VRPA calculations [52], but also considering the range ($\lambda_{min} = 300$ nm and $\lambda_{max} = 600$ nm), as most complexes show noticeable absorption bands in the visible.

$$k = \frac{\int_{\lambda min}^{\lambda max} \varepsilon_\lambda I_\lambda d\lambda}{\int_{\lambda min}^{\lambda max} I_\lambda d\lambda} \tag{12}$$

The VRPA (expressed in W) was calculated according to Eq. (13),

where C is the concentration of iron in solution (0.089 mM), I_0 is the irradiance at the reactor surface, which was 25 W·m^{-2} for the UVA region and 128 W·m^{-2} for the 300–600 nm range, x is the distance from the surface of the liquid to the considered point, accounting from 0 to the depth the liquid (0.07 m), finally, the surface of the reactor (S_r) was 0.0034 m^2.

$$VRPA = S_r \int_0^x k \cdot C \cdot I_0 \cdot 10^{-k \cdot C \cdot x} dx \quad (13)$$

3. Results and discussion

3.1. Effect of ring substitution

3.1.1. Effect of the position of -hydroxyl substituents: dihydroxybenzenes

Three different dihydroxybenzenes, CAT, RES and PHQ, with ortho-, meta- and para- substitution, respectively, were individually added to the photo-Fenton mixture in parallel reactions. A plot of the removal of the mixture of pollutants (expressed as $\Sigma(C/C_0)$) vs. time can be found in Fig. 2.

It can be observed that a process enhancement has been achieved in all three cases when compared with photo-Fenton in the absence of the phenolic compounds, in line with results reported in literature [34,35,53–55]. According to Eqs. (1)–(6) (see introduction), at pH = 5, Fenton inactivation occurs; in contrast, the presence of other ligands able to compete with OH^- (L = CAT, RES or PHQ, in this case) shifts the process towards Eqs. (6)–(7). However, in order to drive this alternative route (photo-Fenton-like process), the Fe-L complex has to be able to reduce iron(III) into iron(II) (Eq. (7)).

Interestingly, notable differences in the performance of photo-Fenton can be found depending on L, following the trend CAT > PHQ > RES. This can be attributed to two factors: a) differences in the stability of the Fe-L complexes and b) the ability of Fe-L to participate in electron transfer processes, regenerating Fe(II). Regarding the first factor, the relative position of the two -OH groups seems to be important, as the *ortho*- substituents can chelate iron more easily, acting CAT as a bidentate ligand [56], while for PHQ and RES formation of bidentate complexes is sterically hindered and more labile monodentate complexes are formed.

On the other hand, the oxidation of the phenols to form semiquinones and quinones could be hypothesized as the step to regenerate Fe(II) from Fe(III) [34,35,41]. In this context, formation of *o*-benzoquinone and *p*-benzoquinone, from CAT and PHQ respectively, is favoured while 1,3-benzoquinone, which would be the product formed from RES, is not a stable compound. Putting all together, CAT is efficient at complexing and reducing Fe(III), PHQ is able to reduce Fe(III) but is a weak ligand whereas RES is both a weak iron ligand and a poor iron reducing agent, thus explaining the observed trends in Fig. 2.

3.1.2. Effect of the number of -hydroxyl substituents

The effect of the number of -OH moieties in the phenolic compound was tested by studying the degradation of the mixture of the six pollutants by photo-Fenton in the presence of PHE, CAT and GAL, having respectively one, two and three -hydroxyl groups attached to the aromatic ring. Fig. 3 shows that all three played a favourable role, although considerable differences can be found among them: in the presence of GAL (with 3 -OH) and CAT (with 2 -OH), removals of 95% and 90% were obtained in 2 min, while 70% removal was obtained for PHE at the same reaction time. This can be explained by taking into account that two -OH in -ortho position are required to form bidentate chelates (CAT and GAL) that are preferred vs. the monodentate complex formed by PHE. Furthermore, -OH moieties are able to activate the aromatic ring as electron donor, thus favouring the electron transfer between Fe(III) and the ligand to regenerate Fe(II).

3.1.3. Effect of phenolic acids

Experiments were performed in the presence of phenolic acids, namely PHB, PRO and GAA, having one, two and three -OH moieties, in addition to the carboxylic group. Although the same trend was observed, GAA > PRO > PHB (Fig. 4), ruled by the number of -OH, the comparison of Figs. 3 and 4 shows that the performance was worsened when compared with the corresponding phenolic compound (PHE > PHB, CAT > PRO and GAL ≥ GAA), and interestingly, PHB played a slight detrimental effect. This might be attributed to the electron withdrawing role of -COOH that decreases the availability of electrons of the aromatic moiety and makes more unlikely the transfer of an electron to Fe(III).

3.1.4. Comparison of -OH vs. -COOH moieties

Another set of experiments was carried out to assess the effect of the nature of the *o*-substituents, as both carboxylic and hydroxyl groups can act as bidentate ligands for iron. For this purpose, CAT (two -OH), SAL (one -OH and one -COOH) and PHT acid (two -COOH) were tested. Fig. 5

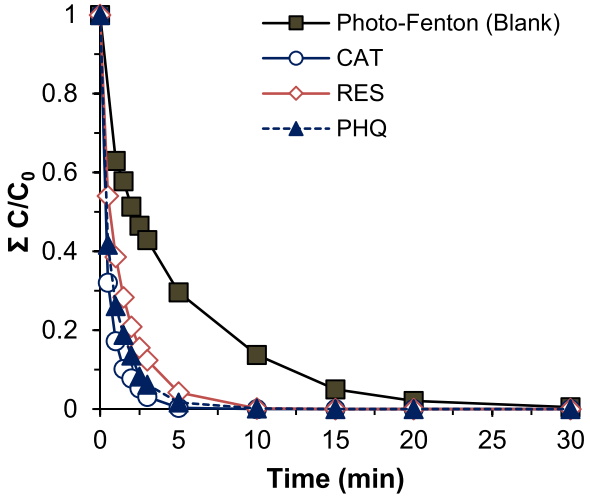

Fig. 2. Photo-Fenton removal of a mixture of six target pollutants (5 mg·L^{-1} each, 30 mg·L^{-1} total concentration) in the presence of 0.227 mmol·L^{-1} of the following complexing agents, according to the hydroxyl group position: catechol (CAT), resorcinol (RES), p-hydroxyquinone (PHQ). Results without complexing agents are also given. Experimental conditions: [Fe(II)] = 0.09 mmol·L^{-1}, [H_2O_2] = 4.29 mmol·L^{-1}, pH = 5.

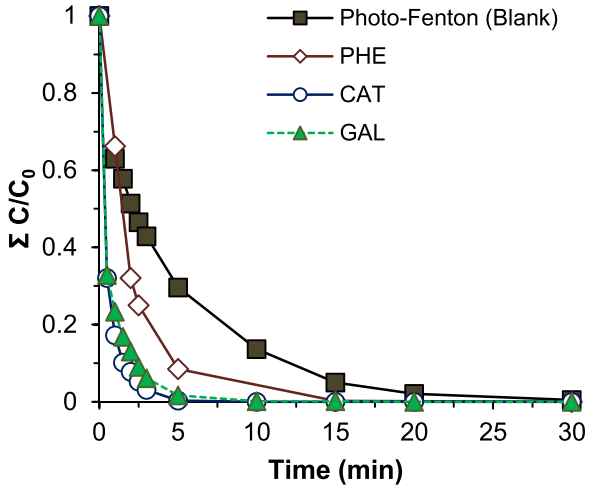

Fig. 3. : Photo-Fenton removal of a mixture of six target pollutants (5 mg·L^{-1} each, 30 mg·L^{-1} total concentration) in the presence of 0.227 mmol·L^{-1} of the following complexing agents, according to the number of -hydroxy substituents: phenol (PHE), catechol (CAT), gallol (GAL). Results without complexing agents are also given. Experimental conditions: [Fe(II)] = 0.09 mmol·L^{-1}, [H_2O_2] = 4.29 mmol·L^{-1}, pH = 5.

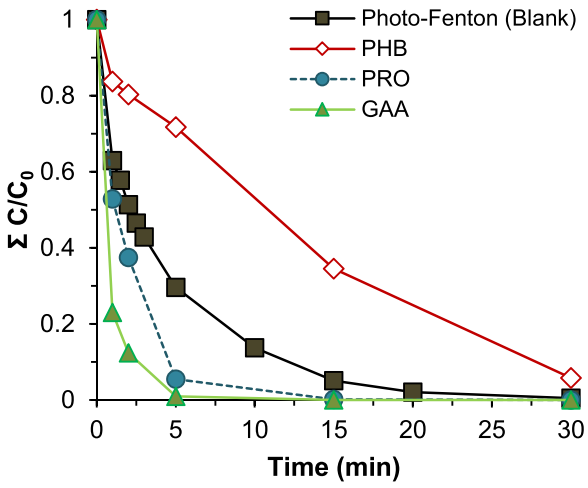

Fig. 4. Photo-Fenton removal of a mixture of six target pollutants (5 mg·L^{-1} each, 30 mg·L^{-1} total concentration) in the presence of 0.227 mmol·L^{-1} of the following complexing agents: phenolic acids according to the number of -hydroxy substituents: p-hydroxybenzoic acid (PHB), protocatechuic acid (PRO), gallic acid (GAA). Results without complexing agents are also given. Experimental conditions: [Fe(II)] = 0.09 mmol·L^{-1}, [H_2O_2] = 4.29 mmol·L^{-1}, pH = 5.

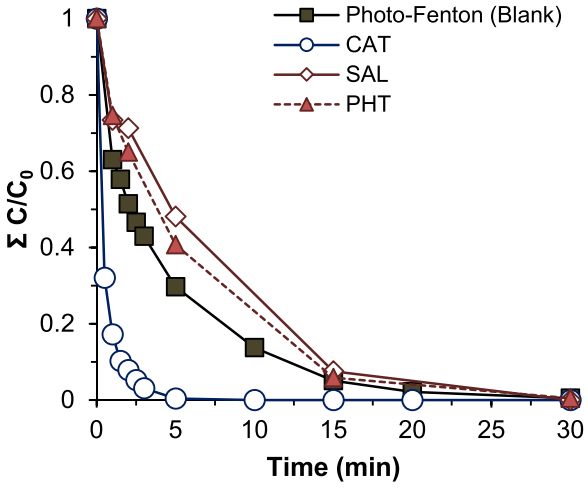

Fig. 5. Photo-Fenton removal of a mixture of six target pollutants (5 mg·L^{-1} each, 30 mg·L^{-1} total concentration) in the presence of 0.227 mmol·L^{-1} of the following complexing agents, divided according to the nature of the *o*-substituents (-OH /-COOH): catechol (CAT), salicylic acid (SAL), phtalic acid (PHT). Results without complexing agents are also given. Experimental conditions: [Fe(II)] = 0.09 mmol·L^{-1}, [H_2O_2] = 4.29 mmol·L^{-1}, pH = 5.

shows that only CAT was able to improve significantly the efficiency of photo-Fenton, while the other two played an inhibitory role, thus indicating that -OH groups are preferred vs. carboxylic ones to regenerate Fe (II).

It is noteworthy indicating that carboxylates have been reported to be excellent ligands to enhance (photo)-Fenton at mild conditions, following a mechanism summarized equations (14−15), where a radical, R·is formed as intermediate. Ligands that follow this mechanism (EDTA, EDDS, NTA, citrate) [14], the formed radical is centred in an aliphatic carbon. However, for benzoic acids (SAL, PHT) an aryl radical would be formed, which exhibits lower stability; thus this pathway is not favoured in this case. On the other hand, ring oxidation to give quinones (as explained for o-diphenols in Section 3.1.1.) is also hindered by the existence of carbon atoms linked to the ring.

$$R\text{-}CO_2^{\cdot} + Fe(III) \rightarrow R\text{-}CO_2^{+} + Fe(II) \quad (12)$$

$$R\text{-}CO_2^{\cdot} \rightarrow R\cdot + CO_2 \quad (13)$$

3.1.5. Comparison of -OH vs. -OCH_3 moieties

Finally, another series of experiments where devoted to compare the behaviour of hydroxyl group (-OH) with that of the methoxyl group (-OCH_3). For this purpose, the efficiency of PRO (two hydroxyl group), VAN (one hydroxyl and one methoxyl group) and VER (two methoxyl groups) was compared. According to Fig. 6, PRO showed the best performance, being the only one able to enhance the process. Again, the presence of two -OH in ortho- position can explain this behaviour. In sharp contrast, VAN and VER played a detrimental role. Although they can act as bidentate ligand and -OCH_3 is an electro-donating moiety that favours the electron transfer, formation of the quinone is hindered by the -OCH_3 bond, what makes these substances inefficient Fe(III) reducing agents.

3.2. Determination of iron regeneration and control experiments

A series of controls were carried out in order to determine the real extent of the photo-Fenton process in the presence of CAT, which was selected as representative ligand from previous experimentation. Fig. 7 shows that pollutants removal was very scarce in all cases, except for (photo)-Fenton, with and without CAT. In these cases, determining the actual effect of irradiation in not easy, as a very fast pollutants removal was observed in the first two minutes of reaction, followed by decrease in the reaction rate. In order to explain this behaviour, the manifold of equations shown in the introduction has to be considered. In the early stages, as iron is added in the form of Fe(II), Eq. (1) is predominating, generating reactive species and Fe(III) with independence of irradiation or iron complexation. On the other hand, as the relative amount of Fe (III) increases, reaction rate is ruled Fe(II) regeneration, which is highly influenced by the ability of photons and/or ligands to reduce Fe(III).

In order to estimate the role of Fenton-(like) in the process (reactions (1−2) and (6−7)), the percentage of removal of the pollutants after 2 min of reaction was calculated according to Eq. (16), where $C_{2\ min}$ is the concentration after 2 min and $C_{15\ min}$ the remaining concentration after 15 min of reaction.

$$\Sigma \text{ CECs removal } (\%) = 100\cdot(1\text{-}C_{15\ min}/C_{2\ min}) \quad (16)$$

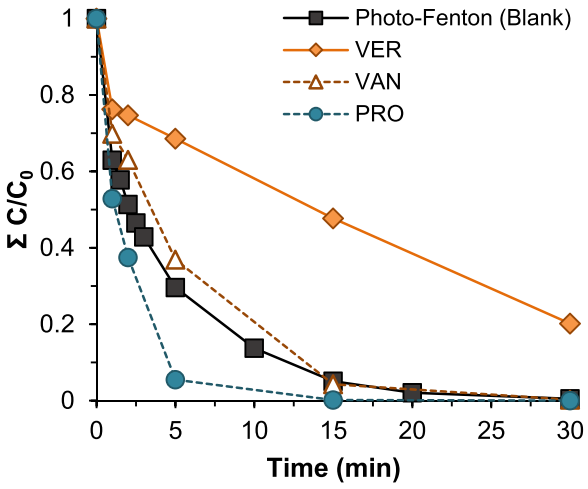

Fig. 6. : Photo-Fenton removal of a mixture of six target pollutants (5 mg·L^{-1} each, 30 mg·L^{-1} total concentration) in the presence of 0.227 mmol·L^{-1} of the following complexing agents, according to hydroxyl group (-OH) and methoxyl group (-OCH_3): veratric acid (VER), vanillic acid (VAN), protocatechuic acid (PRO). Results without complexing agents are also given. Experimental conditions: [Fe(II)] = 0.09 mmol·L^{-1}, [H_2O_2] = 4.29 mmol·L^{-1}, pH = 5.

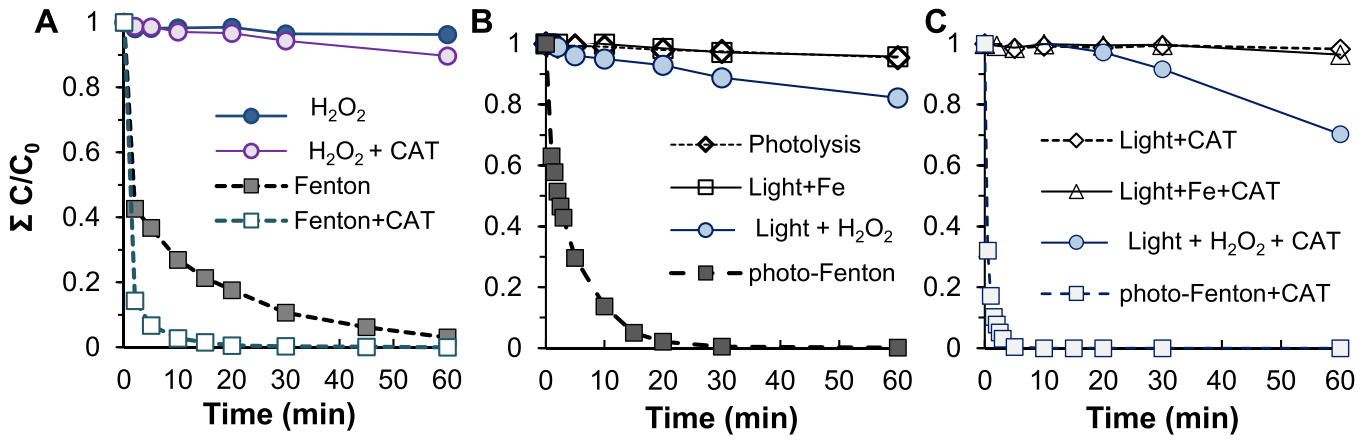

Fig. 7. : Removal of a mixture of six target pollutants (5 mg·L^{-1} each, 30 mg·L^{-1} total concentration) under different processes in dark (A) or irradiated samples in the absence (B) or presence (C) of catechol ([CAT] = 0.227 mmol·L^{-1}). Experimental conditions: [Fe(II)] = 0.09 mmol·L^{-1}, [H_2O_2] = 4.29 mmol·L^{-1}, pH = 5.

These removal (%) values were represented on Fig. 8 for all the phenolics assessed. Thus, Fig. 8 shows that i) most of the ligands can enhance both Fenton and photo-Fenton, ii) better results are systematically obtained upon irradiation and c) the effect of ring substitution above discussed is also valid for Fenton process.

As reduction of Fe(III) within the complex has been suggested as a key step in order to explain the performance of the Fenton reagent in the presence of phenols, this reaction was investigated in more detail. They consisted in determining the formation of Fe(II) in the medium when different ligands were added to a Fe(III) solution. Fig. 9 shows the concentration of Fe(II) that was found after 30 min in each case, which was qualitatively coincident with the trends predicted in the proposed mechanism. The most efficient reduction of Fe(III) into Fe(II) occurred for those ligands having two -OH moieties, following the trend CAT (two –OH in ortho-) > PHQ (two -OH in para-) > PRO (two –OH in ortho- plus a deactivating -COOH moiety). On the other hand, VER and PHT, having two -OMe and -COOH moieties, are unable to reduce efficiently Fe(III), and thus, they play a negative role in the process.

Finally, the ability of the complex to absorb photons might also have some influence on the process. The volumetric rate of photon absorption (VRPA) has been commonly employed to assess the efficiency of the photochemical systems to absorb photons [50,52]. In this regard, VRPA was calculated for Fe(III) and for the complexes formed between iron and the twelve ligands employed, considering the UVA region

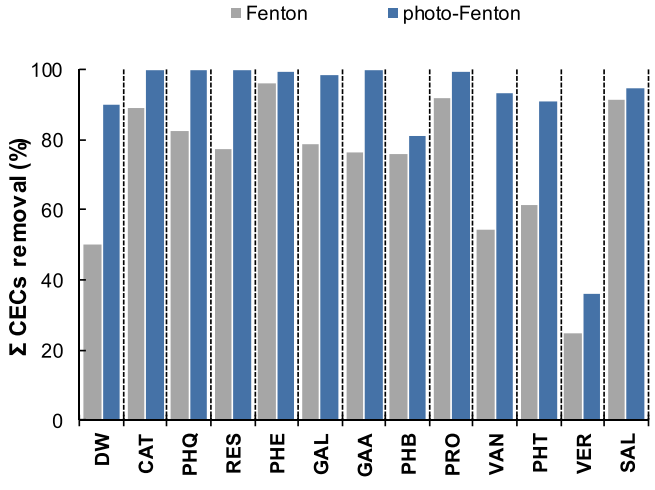

Fig. 8. Σ CECs removal (%) at t = 15 min in Fenton and photo-Fenton process in the presence of selected ligands tested as auxiliaries in this study. Experimental conditions: [Fe(II)] = 0.09 mmol·L^{-1}, [Ligand] = 0.227 mmol·L^{-1}, pH = 5. Results in the absence of ligand are also given (labelled as DW).

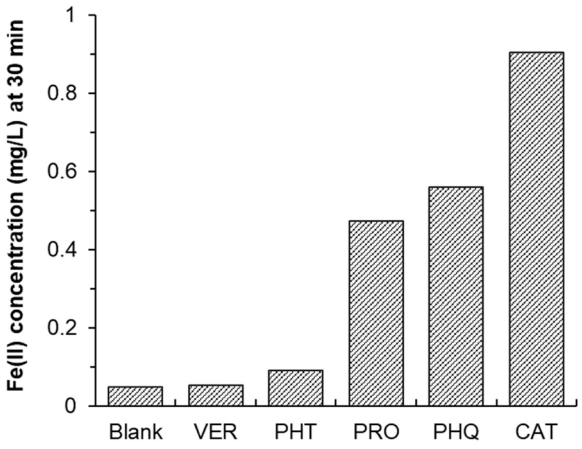

Fig. 9. : Formation of Fe(II) from an Fe(III) solution in the presence of selected ligands tested as auxiliaries for photo-Fenton process. Experimental conditions: [Fe(III)] = 0.09 mmol·L^{-1}, [Ligand] = 0.227 mmol·L^{-1}, pH = 5.

($VRPA_{UVA}$), but also the whole UVA-visible range ($VRPA_{UV–VIS}$). The $VRPA_{UVA}$ for Fe(III) was 0.0332 W, that is comparable to those provided in literature for very similar conditions, considering that the irradiated value was 250 mL in our case [52]; the $VRPA_{UV–VIS}$ for Fe(III) was increased to 0.0893 W.

Table 1 shows the obtained relative values for each ligand ($VRPA_{rel}$), obtained by dividing the corresponding VRPA between that of Fe(III). In

Table 1
VPRA values obtained for the complexes of Fe(III) with the twelve ligands employed in this work. Absolute and relative values are given, considering only the 325–385 nm range ($VRPA_{UVA}$) and also the 300–600 nm range ($VRPA_{UV–VIS}$).

Ligand	$VRPA_{UVA}$ (W)	$VRPA_{UV–VIS}$ (W)	$VRPA_{UVA, rel}$	$VRPA_{UV–VIS, rel}$
Only Fe(III)	0.033	0.089	1	1
CAT	0.022	0.134	0.72	1.45
RES	0.034	0.102	1.01	1.13
PHQ	0.029	0.082	0.89	0.93
PHE	0.034	0.111	1.02	1.21
GAL	0.035	0.174	1.05	1.87
PHB	0.033	0.091	1.00	1.01
PRO	0.034	0.174	1.03	1.87
GAA	0.036	0.187	1.06	2.01
VAN	0.035	0.130	1.05	1.40
VER	0.035	0.114	1.04	1.24
SAL	0.031	0.150	0.95	1.60
PHT	0.033	0.084	0.99	0.95

this way, $VRPA_{rel} > 1$ means an improved absorption of photons. It can be observed that, in general, $VRPA_{UVA,\ rel}$ are close to 1, while $VRPA_{UV-VIS,\ rel}$ are well above 1 in most cases, indicating an increase in the photons absorption because of a shift in the absorption spectrum in the complex towards higher wavelengths. Interestingly, values of $VRPA_{UV-VIS,\ rel} > 1.5$ are reached in most cases for those ligands able to enhance more efficiently the photo-Fenton process (GAA, GAL, PRO); however exceptions can be found as this value is of 0.93 for the highly efficient PHQ-Fe(III) complex. This indicates that photon absorption has a remarkable influence in Fe(III) reduction, but other aspects such as the quantum yields of the inner sphere charge transfer processes, the stability and stoichiometry of the complexes such, as well as the extent of the dark process cannot be neglected. In this context, it has been recently reported that iron complexation by enrofloxacin decreases the photolysis rate of this antibiotic, although the complex shows more intense absorption bands than enrofloxacin alone [57].

3.3. Cross effect of inorganic and organic chelating agents

3.3.1. Combined effect of chlorides and dihydroxybenzenes

In order to check the combined effect of inorganic and organic complexants, experiments were also carried out in water containing different concentrations of chloride, namely 1 $g{\cdot}L^{-1}$ and 30 $g{\cdot}L^{-1}$ (0.017 M and 0.5 M, respectively); CAT, RES and PHQ were used as iron ligands. Fig. 10 shows that all three diphenols were able to enhance the process, and the trend CAT > PHQ > RES was also observed in this case. Interestingly, the positive effect of phenolic compounds was more evident at high salinity (e.g 30 $g{\cdot}L^{-1}$). In fact, high concentrations of chlorides strongly inhibit photo-Fenton in the absence of CAT, RES or PHQ while this inhibition was minimized when these ligands were in solution. This is a key result that opens a promising route for the application of photo-Fenton in highly saline waters, namely seawater.

Iron(III) speciation under different conditions was evaluated according to the mathematical procedure described in Section 2.4, in order to explain the above reported results; CAT was the ligand selected for these calculations. Although there is some dispersion in the values depending on the experimental conditions, the constant for $Fe(OH)^{2+}$ is in the range 10^{-2}-10^{-3} (depending on the ionic strength) [58], this value for $FeCl^{2+}$ is ca. 10 [58], while for CAT the constant is above 10^{40} [49]. The interference of chlorides, is due to changes in the coordination sphere of Fe(III), that prevents formation of $Fe(OH)^{2+}$. Calculations were performed at pH = 5 in MQ water and both concentrations of chlorides, with and without CAT, and also at pH = 2.8, which is the optimum value in MQ water, for the sake of comparison. At pH = 2.8, $Fe(OH)^{2+}$ reaches high concentrations in the absence of chloride (55%, see Table 2), but when chlorides are present, the less efficient chlorinated complexes become predominating (ca. 100%), and a strong inhibition is observed. On the other hand, at pH= 5, inactive $Fe(OH)_2^+$ is predominating (83%) vs $Fe(OH)^{2+}$ (16%), and the presence of chlorides is not so detrimental, as discussed in detail in a previous work [59]. When dihydroxybenzenes are present, these species show a much higher ability to complex iron displacing both, OH^- and Cl^-; this can be observed in speciation in the presence of CAT, as 85% of iron is complexed by this ligand, what accounts for the 100% of the amount of CAT added. This explains that results obtained in the presence of CAT are very similar independently of the water matrix, what means that the relative enhancement by the ligand is more remarkable at high chloride concentrations.

In order to confirm this point, H_2O_2 consumption was determined after 30 min, according to the metavanadate method. Fig. 11 shows that hydrogen peroxide consumption is clearly inhibited by chlorides, in line with results reported in a previous work, attributable to the complexation of iron with chlorides that inhibits the catalytic decomposition of peroxide into reactive species (e.g.·OH). However, when CAT was added to the solution, H_2O_2 consumption was greatly enhanced, in agreement with the hypothesis that CAT replaces chloride and OH^- in the coordination sphere of Fe(III). Interestingly, no significant differences were observed when CAT was present, in the presence and absence of NaCl. Finally, a blank experiment with CAT and hydrogen peroxide in the absence of iron was also performed, showing no consumption of H_2O_2. This means that the increase of peroxide consumption should be attributed to the ability of CAT to keep iron active for photo-Fenton.

3.3.2. Combined effect of fluorides and dihydroxybenzenes

Fluorides forms stronger complexes with Fe(III) than chlorides, as the stability constants are in the order of magnitude of 10^6 for FeF^{2+}, 10^9 for FeF_2^+, and 10^{23} for FeF_3 [57]; hence, it is interesting to compare the effect of both anions on photo-Fenton. Fig. 12A shows that fluorides inhibit photo-Fenton process at pH = 5, both at 1 $g{\cdot}L^{-1}$ and 30 $g{\cdot}L^{-1}$ of NaF, being the effect stronger at this higher concentration. Interestingly, addition of CAT was not able to suppress significantly the inhibitory effect of fluorides, in sharp contrast with observations in the presence of

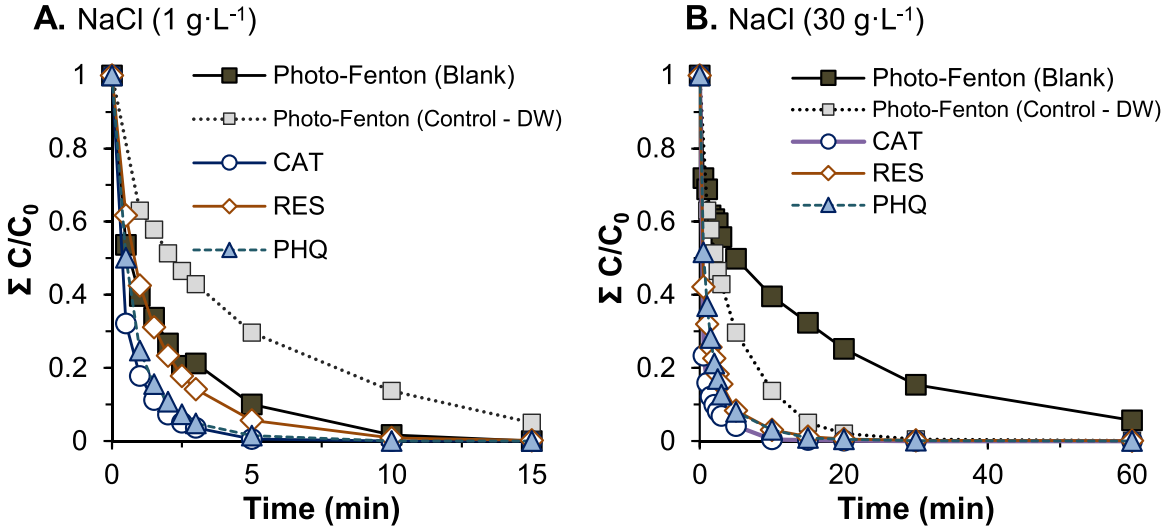

Fig. 10. Photo-Fenton removal of a mixture of six target pollutants (5 $mg{\cdot}L^{-1}$ each, 30 $mg{\cdot}L^{-1}$ total concentration) in two different media: 1 $g{\cdot}L^{-1}$ of NaCl (A) and 30 $g{\cdot}L^{-1}$ of NaCl (B), in the presence of 0.227 $mmol{\cdot}L^{-1}$ of the following complexing agents, according to the hydroxyl group position: catechol (CAT), resorcinol (RES), p-hydroxyquinone (PHQ). Results without complexing agents are also given. Experimental conditions: [Fe(II)] = 0.09 $mmol{\cdot}L^{-1}$, [H_2O_2] = 4.29 $mmol{\cdot}L^{-1}$, pH = 5. DW = Distilled Water.

Table 2
Iron speciation under 9 different experimental conditions. Only those species whose concentration is above 1% are given.

pH	2.8	2.8	2.8	5.0	5.0	5.0	5.0	5.0	5.0
[NaCl] ($g \cdot L^{-1}$)	0	1	30	0	1	30	0	1	30
[CAT] ($mmol \cdot L^{-1}$)	0	0	0	0	0	0	0.227	0.227	0.227
Fe^{3+}	45%	-	-	-	-	-	-	-	-
$Fe(OH)^{2+}$	55%	-	-	16%	1%	-	1%	-	-
$Fe(OH)_2^+$	1%	-	-	83%	35%	-	15%	5%	-
$Fe(OH)_3$	-	-	-	1%	-	-	-	-	-
$FeCl^{2+}$	-	1%	-	-	1%	-	-	-	-
$Fe(Cl)_2^+$	-	99%	100%	-	63%	100%	-	10%	15%
$Fe(CAT)_3^{3-}$	-	-	-	-	-	-	85%	85%	85%

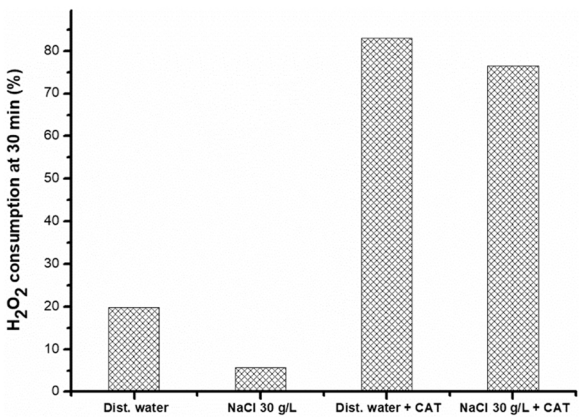

Fig. 11. Hydrogen peroxide consumption after 30 min of photo-Fenton treatment of a mixture of six target pollutants (5 $mg \cdot L^{-1}$ each, 30 $mg \cdot L^{-1}$ total concentration) in distilled water and with 30 $g \cdot L^{-1}$ of NaCl, in the presence/absence of 0.227 $mmol \cdot L^{-1}$ of catechol Experimental conditions: [Fe(II)] = 0.09 $mmol \cdot L^{-1}$, $[H_2O_2]$ = 4.29 $mmol \cdot L^{-1}$, pH = 5.

chlorides. This indicates that CAT cannot replace F^- at these concentrations (molar concentration of fluorides was 3–4 orders of magnitude above that of CAT) while the contrary was true for the more labile Cl^- ligand.

However, these concentrations are well above those commonly found in seawater and are only useful for comparative purposes with the effect of chlorides. As a matter of fact, if the concentration of NaF is decreased to the more realistic value of 40 mg L^{-1}, the molar concentrations of F^- (0.95 mmolar) and CAT (0.227 $mmol \cdot L^{-1}$) are in the same order of magnitude and Fig. 12B shows that this inhibitory effect is suppressed in a higher extent.

4. Conclusions

Some phenolic derivatives have been demonstrated to be useful to enhance photo-Fenton process at pH = 5 via modification of the coordination sphere of iron. In order to play this role, the ligand has to form stable complexes and to be able to reduce Fe(III). Substitution of the aromatic ring is a key parameter, and the presence of at least two -OH moieties enhances the process, being the ortho-position preferred vs. para- and meta- substitutions. On the contrary, rings substituted with -COOH and $-OCH_3$ groups are unable to enhance the Fenton system since, even though they can chelate iron, they are unable to reduce efficiently Fe(III). This systematic study could be of importance in order to correlate the reactivity of macromolecules (e.g humic acids and humic-like substances) with their composition, as well as the number of hydroxyl moieties could be a key parameter. Also extending the investigation to other functional groups (e.g. nitrogenated moieties) is of interest.

Another important issue, is the role of reaction intermediates in the process. Despite a systematic study on the behaviour of ligands has not been carried out, it is clear that they suffer oxidation (e.g. hydroxylation, formation of quinones or ring opening to form linear carboxylic acids), that might have a remarkable influence on the process. Careful detection and quantitation of those products is meaningful, although sophisticated analytical tools might be required.

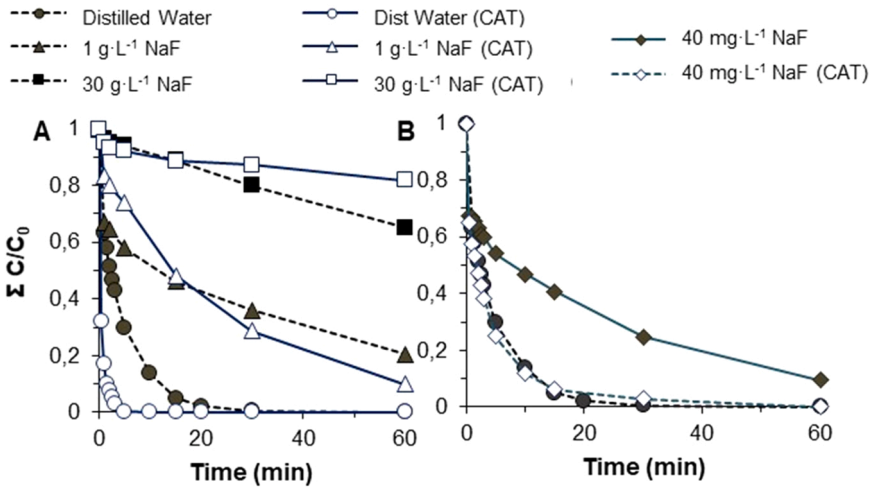

Fig. 12. Photo-Fenton removal of a mixture of six target pollutants (5 $mg \cdot L^{-1}$ each, 30 $mg \cdot L^{-1}$ total concentration) in three different media in the presence/absence of 0.227 $mmol \cdot L^{-1}$ of catechol (CAT). (A) [NaF] = 1 or 30 $g \cdot L^{-1}$; (B) [NaF] = 40 $mg \cdot L^{-1}$. Results without complexing agents are also given. Experimental conditions: [Fe(II)] = 0.09 $mmol \cdot L^{-1}$, $[H_2O_2]$ = 4.29 $mmol \cdot L^{-1}$, pH = 5.

When several species able to complex iron are present in the medium, a competition among them occurs, which is ruled by the stability of the complex as well as the ligand concentration. Thus, slight modification of experimental conditions, or even the nature of the pollutants that are treated, might represent important modifications to the efficiency of photo-Fenton that cannot be neglected. For this reason, further research on the selection of optimal experimental conditions is needed as some negative interferences on the process could be overcome.

Results here reported are very interesting in view of application of photo-Fenton in seawater, taking into account that more than 99% of dissolved iron is bound to organic ligands and that polyphenols are relevant within this pool. This family of organics has been found either in phytoplankton exudates or humic substances, including those tested in the present study such as GAA, CAT, PRO or VAN. Thus, considering the phenolic compounds as an important part of complexing ligands in natural waters, the applicability of Fenton-based processes in such complex waters deserves to be further explored.

It is also necessary to remark that the moieties here studied are present in many pollutants or can be formed as primary by-products. Thus, iron complexation with those pollutants might play a paramount role on their behaviour towards (photo)-Fenton, an aspect that is commonly neglected. Thus, understanding the nature of these effects is of interest in order to prevent reaching misleading conclusions. In those cases, a careful selection of the experiment conditions before applying the process would be especially necessary. For this purpose, a smart modelling of the process would be very useful, considering photons absorption by the photoactive complexes (i.e. using volumetric rate of photon absorption), but also the quantum yields of the inner sphere charge transfer processes, as well as the stability and stoichiometry of the complexes.

CRediT authorship contribution statement

Ivan Vallés: Investigation. **Iván Sciscenko:** Investigation, Conceptualization, Methodology. **Margarita Mora**: Software, Data curation, Formal analysis. **Pau Micó**: Software, Data curation, Formal analysis. **Ana M. Amat**: Writing – review & editing, Project administration, Funding acquisition. **Lucas Santos-Juanes:** Conceptualization, Supervision. **Javier Moreno-Andrés:** Investigation, Conceptualization, Writing – original draft. **Antonio Arques**: Conceptualization, Supervision, Writing – review & editing, Funding acquisition.

Declaration of Competing Interest

The authors declare that they have no known competing financial interests or personal relationships that could have appeared to influence the work reported in this paper.

Data Availability

Data will be made available on request.

Acknowledgments

Authors want to acknoledge the financial support of Spanish Ministerio de Ciencia e Innovación (PID2021-126400OB-C31, AquaEnAgri Project). and TED2021-130994B-C31 and TED2021-130994B-C32 (Ecotranseas). J. Moreno-Andrés acknowledges Grant IJC2020-042741-I funded my MCIN/AEI/10.13039/501100011033 and by the European Union NextGenerationEU/PRTR. I. Sciscenko wants to acknowledge Generalitat Valenciana (CUBackspaceIAPOS/2021/311. I. Vallés ackonowledges Ministerio de Universidades (FPU21/01336)

Appendix A. Supporting information

Supplementary data associated with this article can be found in the online version at doi:10.1016/j.apcatb.2023.122708.

References

[1] H. Luo, Y. Zeng, D. He, X. Pan, Application of iron-based materials in heterogeneous advanced oxidation processes for wastewater treatment: a review, Chem. Eng. J. 407 (2021), 127191.
[2] J. Joseph, S. Iftekhar, V. Srivastava, Z. Fallah, E.N. Zare, M. Sillanpää, Iron-based metal-organic framework: synthesis, structure and current technologies for water reclamation with deep insight into framework integrity, Chemosphere 284 (2021), 131171, https://doi.org/10.1016/j.chemosphere.2021.131171.
[3] Y. Ruan, L. Kong, Y. Zhong, Z. Diao, K. Shih, L. Hou, S. Wang, D. Chen, Review on the synthesis and activity of iron-based catalyst in catalytic oxidation of refractory organic pollutants in wastewater, J. Clean. Prod. 321 (2021), 128924, https://doi.org/10.1016/j.jclepro.2021.128924.
[4] V.K. Sharma, L. Chen, R. Zboril, Review on high valent Fe^{VI} (ferrate): a sustainable green oxidant in organic chemistry and transformation of pharmaceuticals, ACS Sustain. Chem. Eng. 4 (2016) 18–34, https://doi.org/10.1021/acssuschemeng.5b01202.
[5] F. Fu, D.D. Dionysiou, H. Liu, The use of zero-valent iron for groundwater remediation and wastewater treatment: a review, J. Hazard. Mater. 267 (2014) 194–205, https://doi.org/10.1016/j.jhazmat.2013.12.062.
[6] J.A. Donadelli, L. Carlos, A. Arques, F.S. García Einschlag, Kinetic and mechanistic analysis of azo dyes decolorization by ZVI-assisted Fenton systems: pH-dependent shift in the contributions of reductive and oxidative transformation pathways, Appl. Catal. B: Environ. 231 (2018) 51–61, https://doi.org/10.1016/j.apcatb.2018.02.057.
[7] J.J. Pignatello, E. Oliveros, A. MacKay, Advanced oxidation processes for organic contaminant destruction based on the Fenton reaction and related chemistry, Crit. Rev. Environ. Sci. Technol. 36 (2006) 1–84, https://doi.org/10.1080/10643380500326564.
[8] M. Gledhill, K.N. Buck, K.N, The organic complexation of iron in the marine environment: a review, Front. Microbiol. 3 (2012) 1–17, https://doi.org/10.3389/fmicb.2012.00069.
[9] R. Krachler, R.F. Krachler, G. Wallner, S. Hann, M. Laux, M.F. Cervantes Recalde, F. Jirsa, E. Neubauer, F. von der Kammer, T. Hofmann, B.K. Keppler, River-derived humic substances as iron chelators in seawater, Mar. Chem. 174 (2015) 85–93, https://doi.org/10.1016/j.marchem.2015.05.009.
[10] D. Vione, M. Minella, V. Maurino, C. Minero, Indirect photochemistry in sunlit surface waters: photoinduced production of reactive transient species, Chem. Eur. J. 20 (2014) 10590–10606, https://doi.org/10.1002/chem.201400413.
[11] B. Jain, A.K. Singh, H. Kim, E. Lichtfouse, V.K. Sharma, Treatment of organic pollutants by homogeneous and heterogeneous Fenton reaction processes, Environ. Chem. Lett. 16 (2018) 947–967, https://doi.org/10.1007/s10311-018-0738-3.
[12] U.J. Ahile, R.A. Wuana, A.U. Itodo, R. Sha'Ato, R.F. Dantas, R.F, A review on the use of chelating agents as an alternative to promote photo-Fenton at neutral pH: current trends, knowledge gap and future studies, Sci. Total Environ. 710 (2020), 134872, https://doi.org/10.1016/j.scitotenv.2019.134872.
[13] L. Clarizia, D. Russo, I. Di Somma, R. Marotta, R. Andreozzi, Homogeneous photo-Fenton processes at near neutral pH: a review, Appl. Catal. B Environ. 209 (2017) (2017) 358–371, https://doi.org/10.1016/j.apcatb.2017.03.011.
[14] L. Santos-Juanes, Ana M. Amat, Antonio Arques, Strategies to drive photo-Fenton process at mild conditions for the removal of xenobiotics from aqueous systems, Curr. Org. Chem. 21 (2017) 1074–1083, https://doi.org/10.2174/1385272821666170102150337.
[15] P. Soriano-Molina, S. Miralles-Cuevas, I. Oller, J.L. García Sánchez, J.A. Sánchez Pérez, Contribution of temperature and photon absorption on solar photo-Fenton mediated by Fe^{3+}-NTA for CEC removal in municipal wastewater, Appl. Catal. B: Environ. 294 (2021), 120251, https://doi.org/10.1016/j.apcatb.2021.120251.
[16] A.J. Machulek, J.E.F. Moraes Jose, C. Vautier-Giongo, C.A. Silverio Cristina, L. C. Friedrich, C.A.O. Nascimento, M.C. Gonzalez, F.H.Quina Frank, Abatement of the inhibitory effect of chloride anions on the photo-Fenton process, Environ. Sci. Technol. 41 (2007) 8459–8463, https://pubs.acs.org/doi/10.1021/es071884q.
[17] J. Kiwi, A. Lopez, V. Nadtochenko, Mechanism and kinetics of the OH-radical intervention during Fenton oxidation in the presence of a significant amount of radical scavenger (Cl-), Environ. Sci. Technol. 34 (2000) 2162–2168, https://doi.org/10.1021/es991406i.
[18] J. Soler, A. García-Ripoll, N. Hayek, P. Miró, R. Vicente, A. Arques, A.M. Amat, Effect of inorganic ions on the solar detoxification of water polluted with pesticides, Water Res. 43 (2009) 4441–4450, https://doi.org/10.1016/j.watres.2009.07.011.
[19] S. Aguilar, D. Rosado, J. Moreno-Andrés, I. Cartuche, D. Cruz, A. Acevedo-Merino, E. Nebot, Inactivation of a wild isolated Klebsiella pneumoniae by photo-chemical processes: UV-C, UV-C/H_2O_2 and UV-C/H_2O_2/Fe^{3+}, Catal. Today 313 (2018) 94–99, https://doi.org/10.1016/j.cattod.2017.10.043.
[20] J. Bacardit, J. Stötzner, E. Chamarro, S. Esplugas, Effect of salinity on the photo-Fenton process, Ind. Eng. Chem. Res. 46 (2007) 7615–7619, https://doi.org/10.1021/ie070154o.
[21] P. Calza, L. Campra, E. Pelizzetti, C. Minero, Role of H_2O_2 in the photo-transformation of phenol in artificial and natural seawater, Sci. Total Environ. 431 (2012) 84–91, https://doi.org/10.1016/j.scitotenv.2012.05.021.
[22] D. Rubio, E. Nebot, J.F. Casanueva, C. Pulgarin, Comparative effect of simulated solar light, UV, UV/H2O2 and photo-Fenton treatment (UV-Vis/H_2O_2/$Fe^{2+,3+}$) in the Escherichia coli inactivation in artificial seawater, Water Res. 47 (2013) 6367–6379, https://doi.org/10.1016/j.watres.2013.08.006.

[23] R. Yin, Y. Chen, J. Hu, G. Lu, L. Zeng, W. Choi, M. Zhu, Complexes of Fe(III)-organic pollutants that directly activate Fenton-like processes under visible light, Appl. Catal. B: Environ. 283 (2021), 119663, https://doi.org/10.1016/j.apcatb.2020.119663.
[24] I. Sciscenko, S. Garcia-Ballesteros, C. Sabater, M.A. Castillo, C. Escudero-Oñate, I. Oller, A. Arques, Monitoring photolysis and (solar photo)-Fenton of enrofloxacin by a methodology involving EEM-PARAFAC and bioassays: role of pH and water matrix, Sci. Total Environ. 719 (2020), 137331, https://doi.org/10.1016/j.scitotenv.2020.137331.
[25] N. López-Vinent, A. Cruz-Alcalde, J. Giménez, S. Esplugas, C. Sans, Improvement of the photo-Fenton process at natural condition of pH using organic fertilizers mixtures: potential application to agricultural reuse of wastewater, Appl. Catal. B: Environ. 290 (2021), 120066, https://doi.org/10.1016/j.apcatb.2021.120066.
[26] S. Nahim-Granados, I. Oller, S. Malato, J.A. Sánchez Pérez, M.I. Polo-Lopez, Commercial fertilizer as effective iron chelate (Fe^{3+}-EDDHA) for wastewater disinfection under natural sunlight for reusing in irrigation, Appl. Catal. B: Environ. 253 (2019) 286–292, https://doi.org/10.1016/j.apcatb.2019.04.041.
[27] M. Andjelkovic, J. Van Camp, B. De Meulenaer, G. Depaemelaere, C. Socaciu, M. Verloo, R. Verhe, Iron-chelation properties of phenolic acids bearing catechol and galloyl groups, Food Chem. 98 (2006) 23–31, https://doi.org/10.1016/j.foodchem.2005.05.044.
[28] S. García-Ballesteros, M. Mora, R. Vicente, C. Sabater, M.A. Castillo, A. Arques, A. M. Amat, Gaining further insight into photo-Fenton treatment of phenolic compounds commonly found in food processing industry, Chem. Eng. J. 288 (2016) 126–136, https://doi.org/10.1016/j.cej.2015.11.031.
[29] V.J.P. Vilar, M.I. Maldonado, I. Oller, S. Malato, R.A.R. Boaventura, Solar treatment of cork boiling and bleaching wastewaters in a pilot plant, Water Res 43 (2009) 4050–4062, https://doi.org/10.1016/j.watres.2009.06.019.
[30] H. Dong, C. Sans, W. Li, Z. Qiang, Promoted discoloration of methyl orange in H_2O_2/Fe(III) Fenton system: effects of gallic acid on iron cycling, Sep. Purif. Technol. 171 (2016) 144–150, https://doi.org/10.1016/j.seppur.2016.07.033.
[31] H. Dong, Z. Qiang, J. Hu, C. Sans, Accelerated degradation of iopamidol in iron activated persulfate systems: roles of complexing agents, Chem. Eng. J. 316 (2017) 288–295, https://doi.org/10.1016/j.cej.2017.01.099.
[32] Y. Qin, F. Song, Z. Ai, P. Zhang, L. Zhang, Protocatechuic acid promoted alachlor degradation in Fe(III)/H_2O_2 Fenton system, Environ. Sci. Technol. 49 (2015) 7948–7956, https://doi.org/10.1021/es506110w.
[33] P. Villegas-Guzman, S. Giannakis, S.R.A. Torres-Palma, C. Pulgarin, Remarkable enhancement of bacterial inactivation in wastewater through promotion of solar photo-Fenton at near-neutral pH by natural organic acids, Appl. Catal. B Environ. 205 (2017) 219–227, https://doi.org/10.1016/j.apcatb.2016.12.021.
[34] C.L.P.S. Zanta, L.C. Friedrich, A. Machulek, K.M. Higa, F.H. Quina, Surfactant degradation by a catechol-driven Fenton reaction, J. Hazard. Mater. 178 (2010) 258–263, https://doi.org/10.1016/J.JHAZMAT.2010.01.071.
[35] J. Xiao, C. Wang, S. Lyu, H. Liu, C. Jiang, Y. Lei, Enhancement of Fenton degradation by catechol in a wide initial pH range, Sep. Purif. Technol. 169 (2016) 202–209, https://doi.org/10.1016/j.seppur.2016.04.031.
[36] D. Nichela, M. Haddou, F. Benoit-Marquié, M.T. Maurette, E. Oliveros, F.S. García Einschlag, Degradation kinetics of hydroxy and hydroxynitro derivatives of benzoic acid by fenton-like and photo-fenton techniques: a comparative study, Appl. Catal. B Environ. 98 (2010) 171–179, https://doi.org/10.1016/j.apcatb.2010.05.026.
[37] D.A. Nichela, J.A. Donadelli, B.F. Caram, M. Haddou, F.J. Rodriguez Nieto, E. Oliveros, F.S. García Einschlag, Iron cycling during the autocatalytic decomposition of benzoic acid derivatives by Fenton-like and photo-Fenton techniques, Appl. Catal. B Environ. 170–171 (2015) 312–321, https://doi.org/10.1016/j.apcatb.2015.01.028.
[38] J. Gomis, L. Carlos, A. Bianco Prevot, A.S.C. Teixeira, M. Mora, A.M. Amat, R. Vicente, A. Arques, Bio-based substances from urban waste as auxiliaries for solar photo-Fenton treatment under mild conditions: optimization of operational variables, Catal. Today 240 (2015) 39–45, https://doi.org/10.1016/j.cattod.2014.03.034.
[39] S. García-Ballesteros, P. García-Negueroles, A.M. Amat, A. Arques, Humic-like substances as auxiliaries to enhance advanced oxidation processes, ACS Omega 7 (2022) 3151–3157, https://doi.org/10.1021/acsomega.1c05445.
[40] P. Salgado, V. Melin, M. Albornoz, H. Mansilla, G. Vidal, D. Contreras, Effects of pH and substituted 1,2-dihydroxybenzenes on the reaction pathway of Fenton-like systems, Appl. Catal. B: Environ. 226 (2018) 93–102, https://doi.org/10.1016/j.apcatb.2017.12.035.
[41] Y. Pan, R. Qin, M. Hou, J. Xue, M. Zhou, L. Xu, Y. Zhang, The interactions of polyphenols with Fe and their application in Fenton/Fenton-like reactions, Sep. Purif. Technol. 300 (2022), 121831, https://doi.org/10.1016/j.seppur.2022.121831.
[42] V. Kristinova, R. Mozuraityte, I. Storro, T. Rustad, Antioxidant activity of phenolic acids in lipid oxidation catalyzed by different prooxidants, J. Agric. Food Chem. 57 (2009) 10377–10385, https://doi.org/10.1021/jf901072t.
[43] L. Carlos, D.O. Mártire, M.C. Gonzalez, J. Gomis, A. Bernabeu, A.M. Amat, A. Arques, Photochemical fate of a mixture of emerging pollutants in the presence of humic substances, Water Res 46 (2012) 4732–4740, https://doi.org/10.1016/j.watres.2012.06.022.
[44] J.M. Santana-Casiano, M. González-Dávila, A.G. González, F.J. Millero, Fe(III) reduction in the presence of Catechol in seawater, Aquat. Geochem. 16 (2010) 467–482, https://doi.org/10.1007/s10498-009-9088-x.
[45] A. Bernabeu, S. Palacios, R. Vicente, R.F. Vercher, S. Malato, A. Arques, A.M. Amat, Solar photo-Fenton at mild conditions to treat a mixture of six emerging pollutants, Chem. Eng. J. 198–199 (2012) 65–72, https://doi.org/10.1016/j.cej.2012.05.056.
[46] R.F.P. Nogueira, M.C. Oliveira, W.C. Paterlini, Simple and fast spectrophotometric determination of H_2O_2 in photo-Fenton reactions using metavanadate, Talanta 66 (2005) 86–91, https://doi.org/10.1016/j.talanta.2004.10.001.
[47] I. Sciscenko, M. Mora, P. Micó, C. Escudero-Oñate, I. Oller, A. Arques, EEM-PARAFAC as a convenient methodology to study fluorescent emerging pollutants degradation: (fluoro)quinolones oxidation in different water matrices, Sci. Total Environ. 852 (2022), 158338, https://doi.org/10.1016/j.scitotenv.2022.158338.
[48] J. De Laat, T.G. Le, Effects of chloride ions on the iron(III)-catalyzed decomposition of hydrogen peroxide and on the efficiency of the Fenton-like oxidation process, Appl. Catal. B: Environ. 66 (2006) 137–146, https://doi.org/10.1016/j.apcatb.2006.03.008.
[49] N.R. Perron, J.L. Brumaghim, A review of the antioxidant mechanisms of polyphenol compounds related to iron binding, Cell Biochem Biophys. 53 (2009) 75–100, https://doi.org/10.1007/s12013-009-9043-x.
[50] A. Cabrera Reina, L. Santos-Juanes, J.L. García Sánchez, J.L. Casas López, M. I. Maldonado Rubio, G. Li Puma, J.A.S.ánchez Pérez, Modelling the photo-Fenton oxidation of the pharmaceutical paracetamol in water including the effect of photon absorption (VRPA), Appl. Catal. B: Environ. 166–167 (2015) 295–301, https://doi.org/10.1016/j.apcatb.2014.11.023.
[51] https://abet-technologies.com/wp-content/uploads/Sun-2000-Solar-Simulators-2015.pdf.
[52] G. Rivas, I. Carra, J.L. García Sánchez, J.L. Casas López, S. Malato, J.A. Sánchez Pérez, Modelling of the operation of raceway pond reactors for micropollutant removal by solar photo-Fenton as a function of photon absorption, Appl. Catal. B: Environ. 178 (2015) 210–217, https://doi.org/10.1016/j.apcatb.2014.09.015.
[53] F. Chen, W. Ma, J. He, J. Zhao, Fenton degradation of malachite green catalyzed by aromatic additives, J. Phys. Chem. A 106 (2002) 9485–9490, https://doi.org/10.1021/jp0144350.
[54] J. Xiao, C. Wang, H. Liu, Fenton-like degradation of dimethyl phthalate enhanced by quinone species, J. Hazard. Mater. 382 (2020), 121007, https://doi.org/10.1016/j.jhazmat.2019.121007.
[55] J. Moreno-Andrés, L. Vallés, P. García-Negueroles, L. Santos-Juanes, A. Arques, Enhancement of iron-based photo-driven processes by the presence of catechol moieties, Catalysts 11 (2021) 372, https://doi.org/10.3390/catal11030372.
[56] J. Bijlsma, W.J.C. de Bruijn, J.A. Hageman, P. Goos, K.P. Velikov, J.P. Vincken, Revealing the main factors and two-way interactions contributing to food discolouration caused by iron-catechol complexation, Sci. Rep. 10 (2020) 8288, https://doi.org/10.1038/s41598-020-65171-1.
[57] I. Sciscenko, A. Arques, Z. Varga, S. Bouchonnet, O. Monfort, M. Brigante, G. Mailhot, Significant role of iron on the fate and photodegradation of enrofloxacin, Chemosphere 270 (2021) 12979, https://doi.org/10.1016/j.chemosphere.2021.129791.
[58] F.J. Millero, W. Yao, J. Aicher, The speciation of Fe(II) and Fe(III) in natural waters, Mar. Chem. 50 (1995) 21–39, https://doi.org/10.1016/0304-4203(95)00024-L.
[59] I. Vallés, L. Santos-Juanes, A.M. Amat, A.M.J. Moreno-Andrés, A. Arques, Effect of salinity on UVA-Vis light driven photo-Fenton process at acidic and circumneutral pH, Water 13 (2021) 1315, https://doi.org/10.3390/w13091315.